ELSEVIER

Thermochimica Acta 291 (1997) 101–108

thermochimica acta

Transition metal complexes with thiosemicarbazide-based ligands. Part 30. Synthesis, characterization and thermal decomposition of Mo(V, VI) complexes with salicylaldehyde S-methylisothiosemicarbazone

K. Mészáros Szécsényi[a,*], V.M. Leovac[a], E.Z. Iveges̆[a], L. Arman[a], A. Kovács[b], G. Pokol[b], S. Gál[b]

[a] *Faculty of Sciences, Institute of Chemistry, University of Novi Sad, 21000 Novi Sad, Trg D. Obradovica 3, Yugoslavia*
[b] *Institute for General and Analytical Chemistry, Technical University of Budapest, Budapest 1521, Hungary*

Received 4 March 1996; received in revised form 26 July 1996; accepted 9 September 1996

Abstract

The thermal decomposition of several Mo(VI)- and Mo(V)-complexes with salicylaldehyde *S*-methylisothiosemicarbazone (H_2L) of general formula $Mo(VI)O_2(L)$, $Mo(VI)O_2(L)S$ (S = MeOH, EtOH, Py, DMF, DMSO), $(Mo(V)O(HL)Cl)_2O$ and $(Mo(V)O(HL)Cl)_2O{\cdot}Me_2CO$ were investigated. These complexes and the previously prepared Mo(VI) complexes were characterized by spectroscopic (IR, UV–VIS, NMR) and thermal (TG, DTG and DSC) methods. The molar conductivity and magnetic susceptibility of the complexes were also determined. Structure of some decomposition products were determined and a decomposition schemes were proposed. © 1997 Elsevier Science B.V.

Keywords: Molybdenum(V)/(VI)-complexes; Salicylaldehyde *S*-methylisothiosemicarbazone; Thermal decomposition

1. Introduction

Because of the importance of molybdenum in living organisms there are numerous papers and monographs [2,3] concerning the chemistry and role of molybdenum. Molybdenum is an important cofactor of several enzymes catalyzing redox reactions [4]. The mechanism of these reactions has not been completely solved yet. The use of suitable model molecules may be of great help in these studies. The complexes of MoO_2^{2+} with tridentate ligands of general formula $MoO_2(L)S$ (S = solvent molecule) can serve this purpose. These complexes are potential catalysts as the coordinated solvent may be replaced by the activated enzyme molecule. Hence, the desolvation temperature may provide useful information about this process. It has been shown [5,6] that at least one sulphur atom is essential for these complexes to be suitable for model molecules, but the reaction may occur also with the NNN ligands [7]. However, to our knowledge, the catalytic behaviour of complexes with an ONN ligand, to which group belongs salicylaldehyde *S*-methylisothiosemicarbazone, has not been investigated. These complexes are potential candidates for model molecules in further enzyme activity studies.

In a previous paper [1], the synthesis and X-ray characterization of the octahedral cis-dioxo complexes of molybdenum(VI) and tridentate ONN sali-

*Corresponding author. Fax: (381)-21-55-662.

PII S0040-6031(96)03086-9

cylaldehyde *S*-methylisothiosemicarbazone (H_2L) of a general formula $MoO_2(L)S$ (S = MeOH, EtOH, Py) were reported. The present paper deals with the preparation of $(Mo(V)O(HL)Cl)_2OMe_2CO$ and $Mo(V)O(HL)Cl)_2O$ together with $Mo(VI)O_2(L)$ and $Mo(VI)O_2(L)S$ (S = DMF, DMSO) complexes of the same ligand. These complexes and the previously prepared Mo(VI) complexes [1], were characterized by spectroscopic (IR, UV–VIS, NMR) and thermal (TG, DTG and DSC) methods. The molar conductivity and magnetic susceptibility of the complexes were also determined.

2. Experimental

IR spectra of the compounds were recorded in the 450–4000 cm^{-1} range on a Perkin–Elmer 457 spectrophotometer and on a Perkin–Elmer System 2000 FT-IR spectrometer at room temperature using the KBr pellet technique. The latter spectra were obtained with a resolution of 4 cm^{-1} and with the co-addition of 16 scans.

NMR spectra were obtained with a Bruker AC 250 E FT spectrometer operating at 250.13 MHz in a dimethyl-d_6 sulphoxide solvent.

Thermogravimetric measurements were carried out using a DuPont 990 TA system. Sample 4 (~ 5 mg) was heated in a platinum crucible in flowing-air and argon atmospheres to 973 K at a rate of 10 K min^{-1}. All other thermogravimetric measurements were conducted only in flowing air and a heating rate of 10 K min^{-1}.

For DSC measurements, the DSC cell of a DuPont 990 TA system was employed. The samples (~ 5 mg) were weighed in an open aluminium pan, using an empty aluminium pan as reference. Samples were heated at a rate of 10 K min^{-1} in flowing argon. DSC curves were recorded to 623 K.

EGA measurements of samples 7 and 8 were accomplished on a DuPont 916 TEA (Thermal Evolution Analyzer) instrument in flowing nitrogen and a heating rate of 8 K min^{-1} to 600 K. The sample mass was ~ 5 mg.

The molar conductivity of freshly prepared 10^{-3} mol dm^{-3} solutions was measured at room temperature using a digital conductivity meter (Jenway 4010).

Magnetic susceptibility measurements were conducted at room temperature using a magnetic susceptibility balance MSB-MKI, Shewood, Cambridge, UK. The data were corrected for diamagnetic susceptibilities.

3. Results and discussion

3.1. Synthesis, general physico-chemical characteristics and geometry of the complexes

The coordination formulae of the investigated complexes are given in Table 1. The previously described $MoO_2(L)S$ (S = MeOH, EtOH, Py) complexes were prepared by the reaction of warm solutions of $MoO_2(acac)_2$ and H_2L in MeOH, EtOH, or MeOH/Py [1]. The analogous DMF and DMSO

Table 1
Some physico-chemical properties of the complexes

Sample No.	Complex	Colour	μ_{eff} (B.M.)	λ_M (Ω^{-1} cm^2 mol^{-1})
1	$MoO_2(L)$	Orange	diam.	2.2 [a]
2	$MoO_2(L)$MeOH	Orange	diam.	5.6 [a]
3	$MoO_2(L)$EtOH	Orange	diam.	6.1 [a]
4	$MoO_2(L)$DMS	Orange-red	diam.	4.3 [a]
5	$MoO_2(L)$Py	Orange-red	diam.	0.9 [b]
6	$MoO_2(L)$DMF	Orange-red	diam.	5.7 [a]
7	$(MoO(HL)Cl)_2O$	Dark-green	1.64	2.5 [a]
8	$(MoO(HL)Cl)_2O{\cdot}Me_2CO$	Dark-green	1.61	4.1 [b]

[a] MeOH.
[b] Me_2CO.

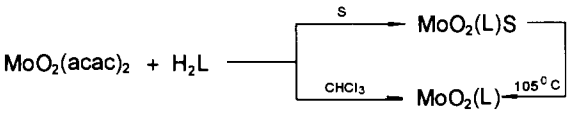

Scheme 1.

complexes were synthesized in a similar way. The desolvated complex $MoO_2(L)$ was made by the reaction of $MoO_2(acac)_2$ and H_2L in $CHCl_3$. It can also be obtained by heating a solvated $MoO_2(L)S$ complex at 380 K to constant mass, as shown in Scheme 1.

The desolvated Mo(V)-complex $(MoO(HL)Cl)_2O$ was prepared by the reaction of warm ethanolic solutions of H_2L and $MoOCl_3$, which was obtained by dissolving $K_2(MoOCl_5)$ and separating the KCl precipitate. The Me_2CO solvate, $(MoO(HL)Cl)_2O{\cdot}Me_2CO$, was prepared by recrystallization of the $(MoO(HL)Cl)_2O$-complex from Me_2CO. The results of the elemental analysis of the newly synthesized complexes were in agreement with the expected values.

All the complexes are crystalline substances, and all lose the solvent completely by isothermal heating at ca. 380 K. The complexes are soluble in DMF, DMSO, Me_2CO and MeOH, less soluble in EtOH, Et_2O and $CHCl_3$ and insoluble in H_2O. Some physico-chemical properties of the complexes are given in Table 1. All the Mo(VI) complexes are diamagnetic, which is in agreement with the d^0 configuration of the central atom. As can be expected, the Mo(V) complexes are paramagnetic with a μ_{eff} that is somewhat less than the spin-only value for the system with $s = 1/2$. Molar conductances of the complexes (Table 1) suggest their nonelectrolytic character resulting from the coordination of H_2L in a dianionic form, i.e. with deprotonation of OH- and NH_2-group [1]. Conversely, for the Mo(V) complexes, this ligand is coordinated as a monanion, via the deprotonated OH-group.

All Mo(VI)-complexes show characteristic IR absorptions in the ranges of 930–940 (ν_s) and 910–895 cm^{-1} (ν_{as}), due to the vibrations of cis-MoO_2 group. The solvated complexes, $MoO_2(L)S$, have an octahedral configuration with the sixth coordination site occupied by a molecule of solvent, which was unambiguously proved by X-ray diffraction analysis [1] of the complexes with MeOH and Py. The newly synthesized complexes with DMF and DMSO have most probably the same structure. The position of $\nu_{(C=O)}$ (1650 cm^{-1}) and $\nu_{(S=O)}$ (995 cm^{-1}) bands in the IR spectra of the DMF and DMSO complexes, respectively, are indicative of the expected coordination of the solvent through oxygen [8,9], as Mo(VI) belongs to hard acids.

For the desolvated $MoO_2(L)$ complex, a less customary pentacoordinated structure can be postulated, because of the absence of absorption due to the Mo=O···Mo bridge [2] at $\sim$ 800 cm^{-1}.

It is most probable that Mo(V) complexes have a μ-oxo-octahedral configuration. The very low λ_M value (Table 1) of these complexes is related to the coordinated chlorine atoms. The Me_2CO solvate, $(MoO(HL)Cl)_2O{\cdot}Me_2CO$, shows a sharp high-intensity IR absorption at 1680 cm^{-1}, due to the $\nu_{(C=O)}$ vibrations of the solvent. The same complex shows a very strong band at 962 cm^{-1} due to trans terminal oxo ligands (Fig. 1). However, the desolvated complex in this range shows two absorption bands of similar intensities, but which are somewhat less intensive compared to the corresponding band of the solvated complex, suggesting a cis-configuration [2] for the desolvated complex. The asymmetric stretching vibrations of the Mo=O···Mo bridge [2] appear at ca. 760 cm^{-1}.

Electronic absorption spectra of Mo(VI) complexes show an absorption maximum at ca. 23 500 cm^{-1} ($\varepsilon = (2.7 - 3.4) \times 10^{-3}$ dm^3 mol^{-1} cm^{-1}) due to CT-type $L \rightarrow M$ transition. The electronic absorption spectral characteristics of Mo(V) complexes are similar to those of Mo(VI) complexes. Hence, the Mo(V) complexes in the visible part of the spectra show no absorption belonging to $d \rightarrow d$ transitions, most prob-

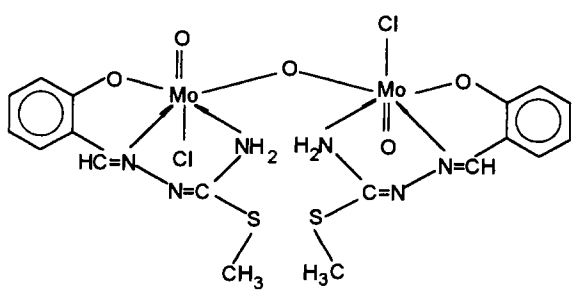

Fig. 1. The proposed structure of the trans-Mo(V) complex.

Table 2
^{1}H and ^{13}C chemical shifts with the assignation to the marked atoms of the Mo-complexes I and II

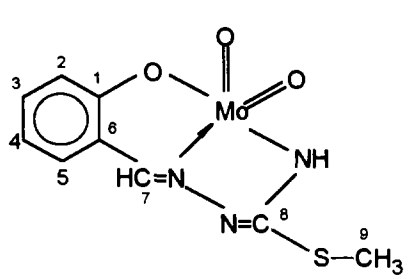

(I)

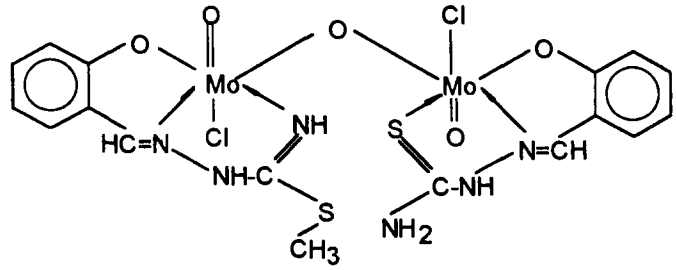

(II)

	δ, ppm								
Atom	1	2	3	4	5	6	7	8	9
I/δ ^{1}H	—	6.83	7.41	6.95	7.59	—	8.52	—	2.47
I/δ ^{13}C	159.86	118.18	133.45	120.31	133.55	120.59	150.73	170.14	14.06
II/δ ^{13}C	159.55	117.99	132.90	119.06	133.49	119.06	150.44	169.76	14.06
	157.32	116.13	132.50	118.56	133.35	118.56	148.12	165.10	—

ably because of the oxidation of Mo(V) to Mo(VI) in the solution. The brown colour of the MeOH solution of Mo(V) complexes is in agreement with this assumption.

The ^{1}H and ^{13}C NMR data of the $MoO_2(L)$, $(MoO(HL)Cl)_2OMe_2CO$ and $(MoO(HL)Cl)_2O$ complexes are presented in Table 2. The resonance of the N–H proton of $MoO_2(L)$ complexes appears at $\delta = 9.17$ ppm. All spectral data are consistent with the given structure.

As the Mo(V) complexes are paramagnetic, the ^{1}H-spectrum of the $(MoO(HL)Cl)_2O{\cdot}Me_2CO$ complex shows a strong signal broadening. Conversely, a partial decomposition of this sample is observed in DMSO-d_6. The presence of only one signal for CH_3-(*S*) in both ^{1}H and ^{13}C NMR spectra of the $(MoO(HL)Cl)_2OMe_2CO$ complex, together with a low-field signal at $\delta = 169.76$ ppm (C=*S*) in ^{13}C NMR spectrum indicated that *S*-demethylation takes place during the experiment. This evidence is strongly supported by the presence of a low-field signal in the ^{1}H NMR spectrum at $\delta = 8.58$ ppm (=N–NH–), confirming thus that one of the =N–N–C= groups is transformed to a =N–NH–C= function. The resonance of one of the $-NH_2$ groups appears at $\delta = 9.65$. To the second $-NH_2$ group belong two signals, most probably because of the $-N{=}C{-}NH_2 \rightarrow -NH{-}C{=}NH-$ transformation ($\delta = 10.45/9.25$ ppm). The signals of all other carbon atoms in the ^{13}C NMR spectrum of Mo(V) complex are duplicated with respect to the signals of the Mo(VI) complex, confirming thus a dimeric structure. The resonance of the C=O from the solvated acetone appears at $\delta = 206.27$ ppm while the signal corresponding to both CH_3-groups appears at $\delta = 30.67$ ppm. The ^{1}H and ^{13}C NMR data of the dissolved $(MoO(HL)Cl)_2O{\cdot}Me_2CO$ complex are in good agreement with structure II in Table 2.

The dissolution of the unsolvated $(MoO(HL)Cl)_2O$ complex in DMSO leads to complete decomposition of the sample, so its NMR spectra are of no use for assignments.

3.2. *Thermal decomposition of samples*

The thermal decomposition of sample 4 was investigated in flowing-air and argon atmospheres. The

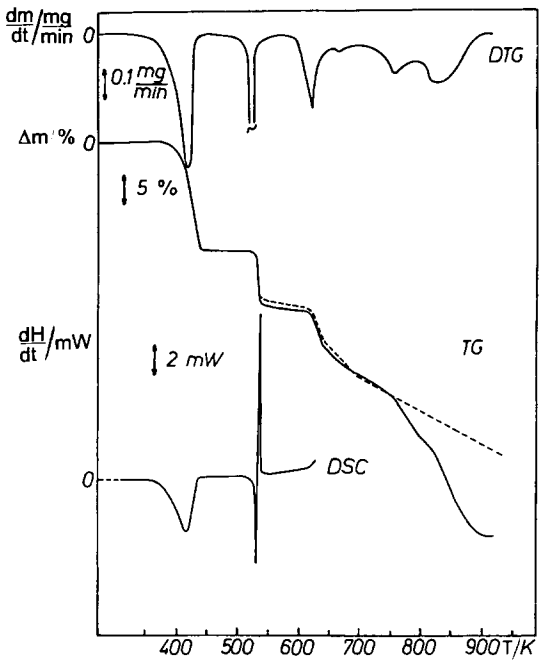

Fig. 2. TG, DTG and DSC curves of $MoO_2(L)$·DMS (heating rate 10 K min^{-1}): – in argon; and – in air.

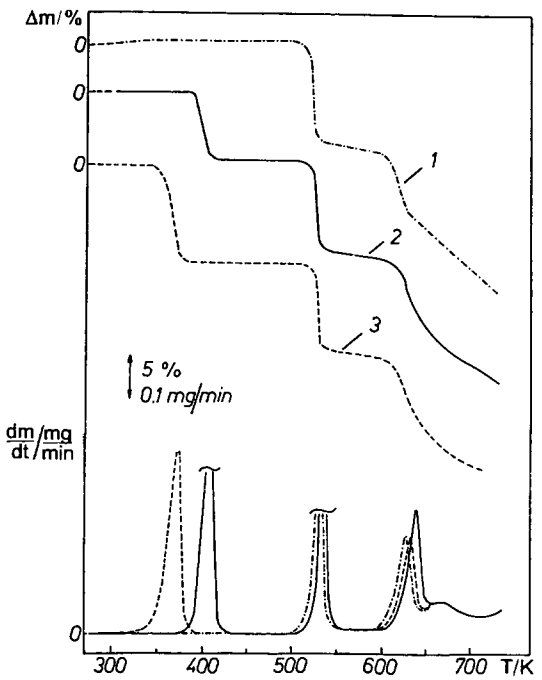

Fig. 3. TG and DTG curves for the samples: 1 – $MoO_2(L)$; 2 – $MoO_2(L)$·MeOH; and 3 – $MoO_2(L)$·EtOH.

corresponding TG, DTG and DSC curves are presented in Fig. 2. The course of the decomposition is similar in both atmospheres to ~ 650 K. In an air, the decomposition of the sample is complete at ~ 900 K with MoO_3 as a final product, while in argon above 650 K, the decomposition rate decreases. All other measurements were carried out in an air.

The TG and DTG curves of samples 1–6 are presented in Figs. 3 and 4 while the DSC curves are shown in Figs. 5 and 6. The first decomposition step is the evaporation of the solvent. In all the cases the solvent is lost in an endothermic process in the 450–340 K range. Samples 5 and 6 contained traces of solvent probably remained after recrystallization. The mass loss for the freshly prepared samples agrees with the composition given by elemental analysis. However, the solvent content of the older samples, as can be seen in Table 2, is somewhat lower.

In the next step, the decomposition of the desolvated complex begins. As expected, the course of decomposition and the decomposition temperature are the same for all the complexes. The process involves a sharp endothermic reaction followed immediately by an exothermic one. The resulting product is relatively stable over a temperature range of ~ 50 K. The mass loss corresponds most likely to the elimination of a molecule of water and dimethyl sulphide from two complex molecules giving a μ-oxo-dimer. The most probable course of the reaction is shown in Scheme 2.

That the reduction of Mo(VI) to Mo(V) occurs is manifested in the paramagnetism of the formed product (μ_{eff} = 0.98 B.M.). The lower value of μ_{eff} with respect to the spin-only value for the system with $s = 1/2$ is a consequence of a dimeric structure. To prove the assumed course of the reaction, the IR spectrum of the product was recorded. Compared with the spectra of the starting compounds the IR spectrum of the product shows significant changes: the NH and SCH_3 vibrations have almost completely vanished from the spectrum of the product. The strong band at 1599 cm^{-1} in the sample spectrum is splitted while the sum of the integrated area of the two peaks (1602 and 1587 cm^{-1}) remained the same compared to the other unchanged bands of the spectra. The 1599 cm^{-1} band in the starting compounds was assigned to the

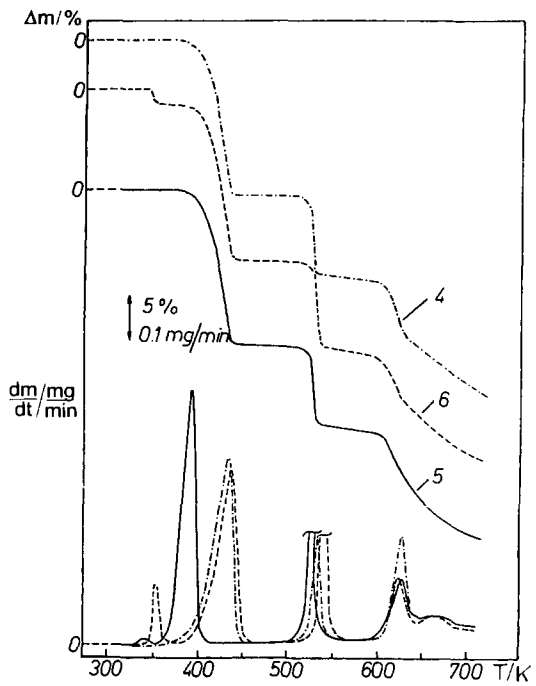

Fig. 4. TG and DTG curves for the samples: 4 – $MoO_2(L)$·DMSO; 5 – $MoO_2(L)$·Py; and 6 – $MoO_2(L)$·DMF.

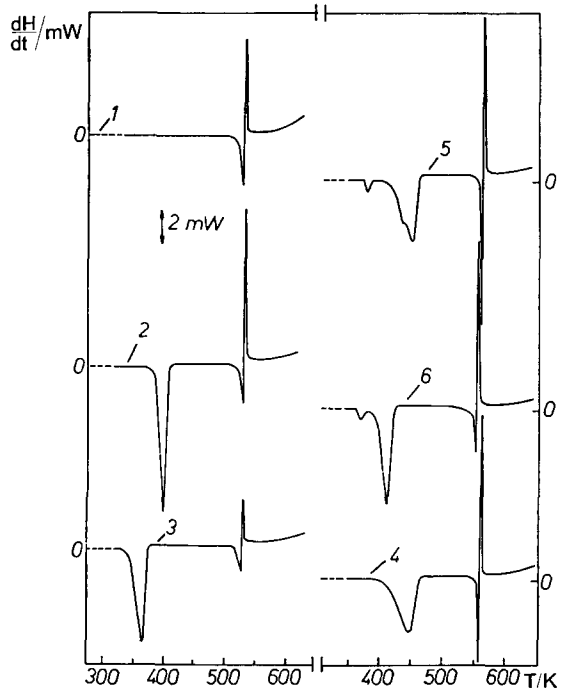

Fig. 5. DSC curves for the samples: 1 – $MoO_2(L)$; 2 – $MoO_2(L)$MeOH; 3 – $MoO_2(L)$·EtOH; 4 – $MoO_2(L)$·DMSO; 5 – $MoO_2(L)$·Py; and 6 – $MoO_2(L)$·DMF.

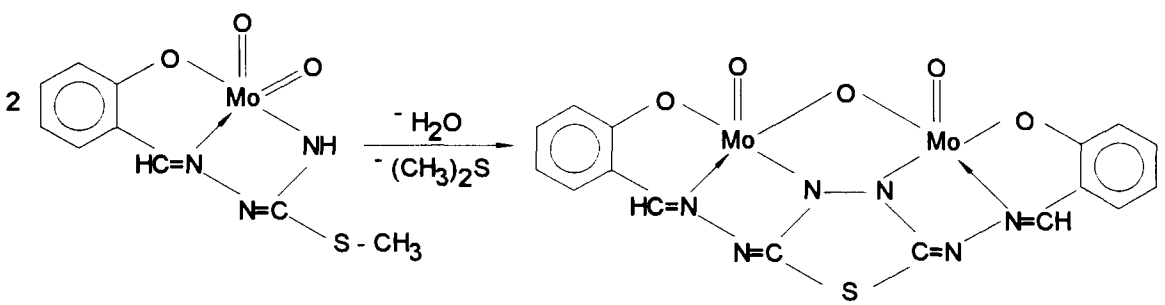

Scheme 2.

overlapping $\nu_{(C=N)}$ and $\nu_{(C=C(Ar))}$ vibrations. The $\nu_{(C=N)}$ vibrations are in general weak, thus the new peak at 1587 cm^{-1} can be attributed to an aromatic $\nu_{(C=C(Ar))}$ vibration. The presence of two aromatic ring vibrations $\sim$ 1600 cm^{-1} indicates a structure involving two aromatic rings. The spectroscopic proof of a dimeric μ-oxo-structure of the decomposition product is the vanishing of the $\nu_{(MoO_2)}$ band from the spectrum and the appearance of bands for $\nu_{(MoOt)}$ and $\nu_{(Mo-Ob-Mo)}$ vibrations at 961 cm^{-1} (sharp, very strong) and 757 cm^{-1} (weak), respectively. These two bands also appear in the spectrum of the decomposition product of the $(MoO(HL)Cl)_2O$·Me_2CO complex. The elemental analysis of the product confirmed the previous assumption. (Calculated for $C_{16}H_{10}N_6O_5SMo_2$ (M_r=590.24): C – 32.5; H – 1.7; O – 13.5; N – 14.2; *S* – 5.4%. Found: C – 32.4; H – 2.2; O – 13.0; N – 11.5, *S* – 8.3%.)

Table 3
Thermal decomposition data for complexes 1–6

Sample No.	Complex	Temperature range (K)	Mass loss (%)		Temperature range (K)	Mass loss (%)		Temperature range (K)	Mass loss (%)	
			found	calculated		found	calculated		found	calculated
1	$MoO_2(L)$	—	—		500–545	12.5	12.05	600–910	59.3	57.06
2	$MoO_2(L)MeOH$	390–420	8.0	8.72	510–550	11.3	11.00	615–915	61.5	60.80
3	$MoO_2(L)EtOH$	340–390	11.5	12.08	510–550	10.1	10.59	610–910	63.7	62.25
4	$MoO_2(L)DMSO$	380–450	18.4	18.90	530–560	10.4	9.77	600–900	67.5	65.18
5	$MoO_2(L)Py$	380–450	18.3	19.09	520–550	9.5	9.75	600–910	65.9	65.26
6	$MoO_2(L)DMF$	360–410	17.3	17.90	510–550	10.0	9.89	600–910	65.1	64.75

In the interval of 590–920 K the complete degradation of the samples occurs with a final product of MoO_3 in the air.

The data for thermal decomposition of Mo(VI) complexes in air for samples 1–6 are given in Table 3.

The only difference between samples 7 and 8, both with Mo(V), is that sample 8 contains additionally a molecule of Me_2CO. However, the thermal decomposition of these samples is completely different (Fig. 6), most probably due to the different (cis/trans) configuration of the complexes.

The endothermic thermal decomposition of sample 7 begins at ~ 540 K with a corresponding mass loss of ~ 2%. The EGA data for this step give an organic carbon degradation product. The mass loss corresponds to the elimination of a CH_4 molecule. A further decomposition follows almost immediately. The DSC curve indicates a rather complex process beginning with an endothermic effect. This is followed by an exothermic reaction that is immediately accompanied by endothermic effects (Fig. 7). The final product of the decomposition is MoO_3. However, the amount of the MoO_3 formed is only half of the expected mass. A possible explanation of this phenomenon is the formation and evaporation of MoO_2Cl_2 while the remaining molybdenum in an air gives one mole of MoO_3 (calculated – 19.79%, found – 20.6%).

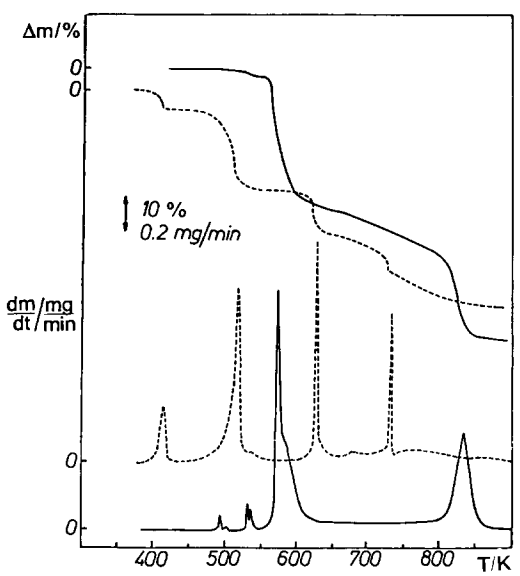

Fig. 6. TG and DTG curves for the samples: – (MoO(HL)Cl)$_2$O·Me$_2$CO; — (MoO(HL)Cl)$_2$O.

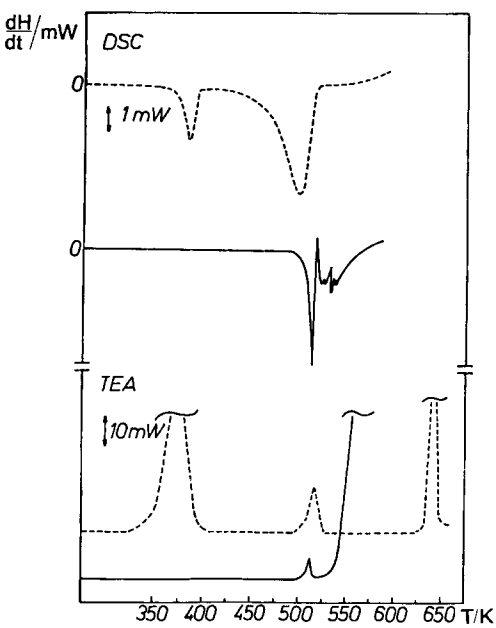

Fig. 7. DSC and EGA curves for the samples: – (MoO(HL)Cl)$_2$O·Me$_2$CO; – (MoO(HL)Cl)$_2$O.

Sample 8 contains a coordinated molecule of acetone which is lost in the interval of 390–420 K (Fig. 6). The amount of the acetone is less than that given by elemental analysis and corresponds to the composition of $(MoO(HL)Cl)_2O{\cdot}0.80Me_2CO$. After the solvent evaporation at $\sim$ 470 K an endothermic mass loss begins. The EGA (Fig. 7) curve of the sample shows an organic decomposition product at the same temperature as in the case of sample 7. However, from this point onwards, the mechanism of further decomposition is completely different (Fig. 6). While sample 7 decomposes completely, sample 8 gives an intermediate product that is almost stable starting at 550 K (up to 600 K). The complete mass loss for the intermediary compound corresponds to the elimination of a CH_4, a CH_3SH and two HCl molecules. The IR spectrum of this compound is identical to the spectrum of the product of the $MoO_2(L)$ decomposition. The degradation is completed at $\sim$ 900 K in the air atmosphere giving two moles of MoO_3 (found – 35.5%, calculated – 36.69%) as a final product.

4. Conclusions

The tridentate ONN ligand of salicylaldehyde *S*-methylisothiosemicarbazone (H_2L) stabilizes molybdenum in +6 and +5 oxidation states giving octahedral $Mo(VI)O_2(L)S$ complexes (S = MeOH, EtOH, DMSO, DMF, Py) and also octahedral μ-oxo dimer $(Mo(V)O(HL)Cl)_2O$, respectively.

The desolvation of the octahedral $Mo(VI)O_2(L)S$ solvate (L = dianion of the salicylidene *S*-methylisothiosemicarbazide ligand) complexes takes place in the 340–450 K range. The product is a desolvated complex with an unusual pentacoordinated structure which is stable to 500 K. In the next step of thermal decomposition a relatively stable μ-oxo-dimer formation occurs. The same product is formed by thermal decomposition of the $(Mo(V)O(HL)Cl)_2O{\cdot}Me_2CO$ solvate. However, the course of thermal decomposition of the desolvated $(Mo(V)O(HL)Cl)_2O$ complex is different. It decomposes completely in the 590–800 K range. The difference in the thermal behaviour of the complexes is due to different configuration of the complexes. The final product of decomposition is MoO_3 in all the cases. However, the amount of MoO_3 formed by decomposition of the desolvated Mo(V)-complex (sample 7) is half of the expected mass, most probable because of formation and evaporation of MoO_2Cl_2.

The high thermal stability of the pentacoordinated Mo(VI)-complex formed by desolvation may refer to a hindered μ-oxo-molybdenum(V) dimer formation in this case.

Acknowledgements

Dr. V. Izvekov, Hungarian National Scientific Research Foundation (OTKA, No. F 014518). This work was supported in part by the Serbian Research Fund.

References

[1] E.Z. Ivegeš, V.M. Leovac, G. Pavlović and M. Penavić, Polyhedron 11 (1992) 1659.
[2] E.I. Stiefel, in S.J. Lippard (Ed.), The coordination and bioinorganic chemistry of molybdenum, Prog. Inorg. Chem., Vol. 22, Wiley-Interscience, New York (1977) pp. 1–223.
[3] E.I. Stiefel, in G. Wilkinson, R.D. Gillard and J. McCleverty (Eds.), Comprehensive coordination chemistry, Molybdenum(VI), Vol. 3, Pergamon Press, Oxford (1987) pp. 1375–1420.
[4] M.P. Coughlan (Ed.), Molybdenum and molybdenum-containing enzymes, Pergamon Press, New York (1980).
[5] J.M. Berg and R.H. Holm, J. Am. Chem. Soc. 107 (1985) 917.
[6] J. Topich and J.T. Lyon III, Inorg. Chem. 23 (1984) 3202.
[7] S.A. Roberts, C.G. Young, C.A. Kipke, W.E. Cleland Jr., K. Yamanouchi, M.D. Carducci and J.A. Enemark, Inorg. Chem. 29 (1990) 3650.
[8] K. Nakamoto, Infrared and Raman spectra of inorganic and coordination compounds, Wiley-Interscience, New York (1986).
[9] V.M. Leovac, I. Ivanović, K. Andelković and S. Mitrevski, J. Serb. Chem. Soc. 60 (1995) 1.